Benchmarks for multicomponent diffusion and electrochemical migration

Rasouli, Pejman; Steefel, Carl I.; Mayer, K. Ulrich; Rolle, Massimo

Published in:
Computational Geosciences

Link to article, DOI:
10.1007/s10596-015-9481-z

Publication date:
2015

Document Version
Peer reviewed version

This is a Post Print of the article published on line 1st May 2015 and printed June 2015 in Computational Geosciences, 19, 523-533. The publishers' version is available at the permanent link: doi:10.1007/s10596-015-9481-z

Benchmarks for multicomponent diffusion and electrochemical migration

Pejman Rasouli[1*], Carl I. Steefel[2], K. Ulrich Mayer[1] and Massimo Rolle[3]

[1]Department of Earth, Ocean and Atmospheric Sciences, University of British Columbia, 2207 Main Mall, Vancouver, BC V6T 1Z4, Canada
[2]Earth Sciences Division, Lawrence Berkeley National Laboratory, Berkeley, CA 94720, USA
[3]Department of Environmental Engineering, Technical University of Denmark, Miljøvej Building 115, 2800 Kgs. Lyngby, Denmark
*corresponding author: prasouli@eos.ubc.ca

Abstract

In multicomponent electrolyte solutions, the tendency of ions to diffuse at different rates results in a charge imbalance that is counteracted by the electrostatic coupling between charged species leading to a process called "electrochemical migration" or "electromigration". Although not commonly considered in solute transport problems, electromigration can strongly affect mass transport processes. The number of reactive transport models that consider electromigration has been growing in recent years, but a direct model inter-comparison that specifically focuses on the role of electromigration has not been published to date. This contribution provides a set of three benchmark problems that demonstrates the effect of electric coupling during multicomponent diffusion and electrochemical migration and at the same time facilitates the inter-comparison of solutions from existing reactive transport codes. The first benchmark (Lichtner, 1995) focuses on the 1D-transient diffusion of HNO_3 (pH = 4) in a NaCl solution into a fixed concentration reservoir, also containing NaCl - but with lower HNO_3 concentrations (pH = 6). The second benchmark describes the 1D steady-state migration of the sodium isotope ^{22}Na triggered by sodium chloride diffusion in neutral pH water. The third benchmark (Rolle et al., 2013) presents a flow-through problem in which transverse dispersion is significantly affected by electromigration. The system is described by 1D transient and 2D steady-state models. Very good agreement on all of the benchmarks was obtained with the three reactive transport codes used: CrunchFlow, MIN3P and PHREEQC.

Keywords: Reactive transport modeling, multicomponent diffusion, electromigration, model intercomparison, benchmark

1. Introduction

It is well known that diffusive transport in multicomponent electrolyte systems cannot be fully described by Fickian diffusion alone, but is affected by a variety of processes including the electrostatic interactions between individual ions (Vinograd and McBain, 1941; Newman, 1973; Ben-Yaakov, 1981; Cussler, 1997). Each dissolved species is subject to its own species-dependent diffusion coefficient, affected by parameters such as charge and size of the ion (Cussler, 1997) and ionic conductivity (Lasaga, 1979). As a result, dissolved species will tend to diffuse at different rates, promoting the development of a charge imbalance in solution. However, positively and negatively charged species are also affected by electric coupling, which ensures that charge balance in solution is maintained. Generally speaking, "large" cations and "small" anions are tied together electrostatically (Newman, 1973; Cussler, 1997) to enforce electroneutrality at the macroscale - an essential condition in electrolyte solutions (Lichtner, 1996; Van Cappellen and Gaillard, 1996). This electric coupling leads to an additional mass transport process called "electrochemical migration" or "electromigration" (Newman, 1991; Ben-Yaakov, 1981). Fick's law neglects these interactions, describes ion migration solely based on concentration gradients, and consequently does not consider the electric field generated by electrostatic bonding (coulombic interactions) of charged species (Lasaga, 1979; McDuff and Ellis, 1979; Newman, 1991; Lichtner, 1996; Van Cappellen and Gaillard, 1996). In a multicomponent system that includes charged species, diffusive ion migration is therefore better described by the Nernst-Plank equation, a formulation that explicitly considers the electric coupling between species and ensures the conservation of charge (Lasaga, 1979; McDuff and Ellis, 1979; Newman, 1991; Lichtner, 1996; Van Cappellen and Gaillard, 1996; Boudreau et al., 2004; Liu et al., 2011; Steefel et al., 2014).

In some cases, electrostatic interactions between diffusing species can have a strong effect on ion mobility and can produce unexpected behavior such as uphill diffusion (e.g.: Oelkers, 1996). In addition, apparent diffusion coefficients (i.e. diffusion coefficients derived from Fick's law) may show a strong dependency on concentrations. Considering that the quantification of diffusion coefficients is labor-intensive (Tyrell, 1961; Cussler, 1997), it is impractical to determine apparent diffusion coefficients as a function of solution composition for a range of conditions. Instead, it is advantageous to consider electrochemical interactions affecting diffusion explicitly rather than lumping this effect into empirically measured apparent diffusion coefficients.

Reactive transport models are commonly used for the quantitative investigation of flow, transport and reaction processes in porous media. These models aid with the verification of conceptual models, are used to design and evaluate experiments, and assist with the interpretation of field data in the fields of geology, engineering and environmental research (Boudreau, 1997; Kang et al. , 2006; Steefel et al., 2003; Wang and Van Cappellen, 1996; MacQuarrie and Mayer 2005). Traditionally, diffusion has been implemented into reactive transport models based on Fick's law and diffusion coefficients are often treated as adjustable parameters (Cussler, 1997). However, the number of reactive transport models that include electromigration and consider the chemical potential gradient as the driving force of diffusion has been growing in recent years (Parkhurst and Appelo, 1999; Giambalvo et al., 2002; Shiba et al., 2005; Johannesson et al 2007; Paz-Garcia et al., 2011; Muniruzzaman et al., 2014). Although some aspects of electromigration on solute transport have been investigated (Oelkers, 1996; Giambalvo et al., 2002; Steefel and Maher, 2009), a direct model inter-comparison that

specifically focuses on the role of electromigration and electrostatic effects on ion transport has not been published to date.

This contribution was motivated by the need for benchmark problems suited to evaluate the effect of electric coupling during multicomponent diffusion and electrochemical migration and to facilitate an inter-comparison of existing reactive transport codes. The following benchmark problems are specifically designed to highlight effects of electromigration. The first two benchmarks are one-dimensional and the third benchmark includes two parts, involving one- and two-dimensional scenarios. Three reactive transport codes were used independently for the inter-comparison, namely CrunchFlow (Steefel et al., 2014), MIN3P (Mayer et al., 2002) and PHREEQC (Parkhurst and Appelo, 1999).

2. Governing Equations

Mass Transfer in Electrolytic Systems

Species-specific diffusion is necessary to describe the behavior of electrolyte systems (Steefel and Maher, 2009) where diffusive transport is the dominant mass transport process. The most important feature that distinguishes the electrolyte systems from non-electrolyte systems is the electric coupling of the ionic fluxes (Helfferich, 1962; Newman, 1973). In the electrolyte systems, electric interaction of ion-ion, ion-solvent and ion-interface induces an electric field. The treatment of electrolytic diffusion follows naturally from the generalized treatment of diffusion (Taylor and Krishna, 1993).

Nernst-Planck Equation for Multicomponent Systems

The migration of interacting species is described by the Nernst-Planck equation, which can be derived from expressions for the diffusive flux written in terms of the chemical potential (Steefel

et al, 2014). Written in terms of the flux of an arbitrary species *i*, the Nernst-Planck equation is given by:

$$\mathbf{J}_i = -D_i\left(\nabla c_i + c_i \nabla \ln\gamma_i + \frac{c_i F}{RT} z_i \nabla\psi\right) \qquad (1)$$

where D_i is the species-dependent diffusion coefficient ($m^2\ s^{-1}$), c_i is the concentration (mol L^{-1} H_2O), γ_i is the activity coefficient (-), F is the Faraday constant (96485 C mol^{-1}), R is the gas constant (8.341 J K^{-1} mol^{-1}), T is the absolute temperature (K), z_i is the charge number (-) and ψ is the electric potential (V or J C^{-1}). In the presence of advection with a Darcy's velocity **q** (m s^{-1}), the modified flux term is:

$$\mathbf{J}_i = -D_i\left(\nabla c_i + c_i \nabla \ln\gamma_i + \frac{c_i F}{RT} z_i \nabla\psi\right) + c_i \mathbf{q} \qquad (2)$$

This expression is known as the extended Nernst-Planck equation and holds, in ideal systems, for all mobile species. It describes the movement of ions in a solution with or without external electric field (Helfferich, 1962, Bard, 1980 and Bagotsky, 2006). In a multicomponent system, the set of Nernst-Planck equations, one for each species, must be solved simultaneously.

By assuming small gradients in ionic strength, a dilute solution with low ionic strength and isothermal conditions, the contribution of the flux from the gradients in the logarithms of the activity coefficients can be neglected (Giambalvo et al., 2002; Steefel and Maher, 2009). With this approximation, the flux of an individual species becomes:

$$\mathbf{J}_i = -D_i\left(\nabla c_i + \frac{c_i F}{RT} z_i \nabla\psi\right) + c_i \mathbf{q} \qquad (3)$$

This equation represents the contributions of diffusion, electromigration and advection to the total mass transfer. Assuming there is no externally induced current (null current assumption), a simplified version of the mass flux can be derived (Giambalvo et al., 2002):

111 $$\mathbf{J}_i = -D_i \left(\nabla c_i + c_i z_i \frac{\mathbf{q} \sum_j^{N_{aq}} z_j c_j - \sum_k^{N_{aq}} D_k z_k \nabla c_k}{\sum_l^{N_{aq}} D_l z_l^2 c_l} \right) + c_i \mathbf{q} \qquad (4)$$

112 This formulation has the advantage that the electric potential does not appear as a primary
113 unknown and is therefore well suited for implementation in standard reactive transport codes.

114 3. Participating Codes

115 The three reactive transport codes participating in this benchmarking exercise are CrunchFlow
116 (Steefel et al., 2014), MIN3P (Mayer et al., 2002) and PHREEQC (Parkhurst and Appelo, 1999).
117 CrunchFlow and MIN3P are 3D block-centered finite difference (finite volume) models using
118 the global implicit approach (GIA) to solve the fully coupled transport and reaction equations.
119 PHREEQC solves the multicomponent diffusion problem with a 1D finite difference method
120 using the sequential non-iterative approach (SNIA). A detailed description of the formulation
121 and capabilities of the codes is discussed elsewhere (Steefel et al., 2014 and references therein).
122 PHREEQC considers the gradients of the activity coefficients in its implementation (Appelo and
123 Wersin, 2007) whereas CrunchFlow and MIN3P neglect this contribution.

124 4. Benchmark Descriptions

125 The three benchmark problems are summarized in **Table 1**. The first benchmark (Benchmark 1)
126 focuses on the role of electromigration in driving the flux of the various charged species to
127 maintain local charge balance and was first presented by Lichtner (1995). This problem
128 considers diffusion of HNO_3 from a low pH solution (pH = 4) into a circum-neutral reservoir (pH
129 = 6) with low HNO_3 concentrations, both with the same elevated NaCl background
130 concentrations.

Table 1. Summary of multicomponent diffusion benchmarks

Benchmark	Description	Processes	Dimension
1	HNO_3 (pH 4) diffusion into a circum-neutral pH reservoir	Diffusion/Electromigration	1D
2	Sodium isotope fractionation induced by sodium chloride diffusion in neutral pH water	Diffusion/Electromigration	1D
3	Transverse dispersion affected by electromigration	Advection/Diffusion/ Electromigration	1D/2D

The second benchmark (2) shows the electromigration and subsequent fractionation of the sodium isotope $^{22}Na^{+}$ due to diffusion of NaCl under neutral pH conditions. The problem is loosely based on Glaus et al (2013); however, the benchmark case presented here is set up for a uniform relatively coarse-grained uncharged porous medium and does not include diffusion through charged micropores as would be the case if porous clay were considered. In the first two benchmarks, diffusion and electromigration are the only transport processes and models are set up in one dimension. The third benchmark (3) investigates the effect of electromigration on transverse dispersion and is based on experiments and modeling carried out by Rolle et al. (2013). This benchmark also includes advection and is characterized by a higher level of complexity; it is simulated in one- and two-dimensions.

Benchmark 1: Transient Electromigration

This problem was initially presented by Lichtner (1995) and has previously been used as an example to illustrate the multicomponent capabilities of PHREEQC (Appelo, 2007). It is a 1D transient problem with a fixed concentration (Dirichlet) boundary condition on the left (at x = 0),

representing the reservoir, and a no-flux (Neumann) boundary condition on the right (x = 0.01 m). The chemical system is composed of four primary (component) species (H^+, NO_3^-, Na^+ and Cl^-) and one secondary species (OH^-). The porosity is set to 1.0 and the domain is discretized into 100 equally spaced cells of 100 microns each. The temperature is 25ºC and there is no flow, the only transport process is multicomponent diffusion according to the Nernst-Planck equation. Activity coefficients are calculated with the extended Debye-Hückel equation. Species-dependent diffusion coefficients, as well as the initial and boundary conditions defining the chemical system are given in **Table 2**.

Table 2. Boundary conditions, initial conditions, and species dependent diffusion coefficients for Benchmark 1 (transient electromigration problem).

Species	Boundary Condition (mM)	Initial Condition (mM)	Diffusion Coefficient ($m^2\ s^{-1}$)
pH	6.001	4.007	9.31×10^{-9}
Na^+	0.1	0.1	1.33×10^{-9}
Cl^-	0.1	0.1	2.03×10^{-9}
NO_3^-	0.001	0.1	1.90×10^{-9}
OH^-	[a] 1.03×10^{-5}	[a] 1.06×10^{-7}	5.27×10^{-9}

[a] OH- concentrations are only provided for completeness, calculated from H^+ and H_2O ($K_w = 10^{-14}$)

The problem is run for 1 hour using a constant time step of 0.001 hour (corresponding to 1,000 time steps). Results are compared along the spatial profile after T = 1 hour for H^+, Na^+, NO_3^- and Cl^-.

Benchmark 2: Tracer Isotope Diffusion

This 1D problem involves three primary (component) species, Na^+, Cl^-, and H^+, along with an isotope of Na that is also treated as a distinct component, $^{22}Na^+$. In addition, a single secondary species, OH^-, is considered. In this case, fixed concentration (Dirichlet) boundary conditions are considered at either end of the domain. The initial condition in the domain is divided into two

regions; concentrations in half of the domain are equivalent to those at the left boundary, while concentrations in the other domain half are defined by the right boundary condition. However, the initial conditions are not significant since the simulation is run until steady state conditions are achieved. The porosity is set to a constant and uniform value of 0.5 and the domain is discretized into 100 equally spaced cells of 100 microns each. The diffusion coefficients of Na^+ and $^{22}Na^+$ are assumed to be identical. A constant time step of 1 hour is used and the simulation is run to 1,500 days to ensure that steady-state is achieved. Concentrations at the boundaries and species-dependent diffusion coefficients are described in **Table 3**. The simulation also assumes no flow.

Table 3. Boundary conditions and diffusion coefficients for Benchmark 2 (isotope tracer problem).

Species	Left Boundary Condition (mM)	Right Boundary Condition (mM)	Diffusion Coefficient ($m^2\ s^{-1}$)
pH	7.0	7.0	9.31×10^{-9}
Na^+	0.5	0.1	1.33×10^{-9}
$^{22}Na^+$	10^{-6}	10^{-6}	1.33×10^{-9}
Cl^-	0.5	0.1	2.03×10^{-9}
OH^-	[a]1.05×10^{-4}	[a]1.03×10^{-4}	5.27×10^{-9}

[a]OH- concentrations are only provided for completeness, calculated from H^+ and H_2O ($K_w = 10^{-14}$)

Benchmark 3: Transverse Dispersion

Rolle et al. (2013) investigate the effect of electromigration on transverse dispersion under steady state flow conditions. In the full 2D case, the problem involves unidirectional flow and transport of a multicomponent tracer plume down the length of a 2D flow-through chamber.

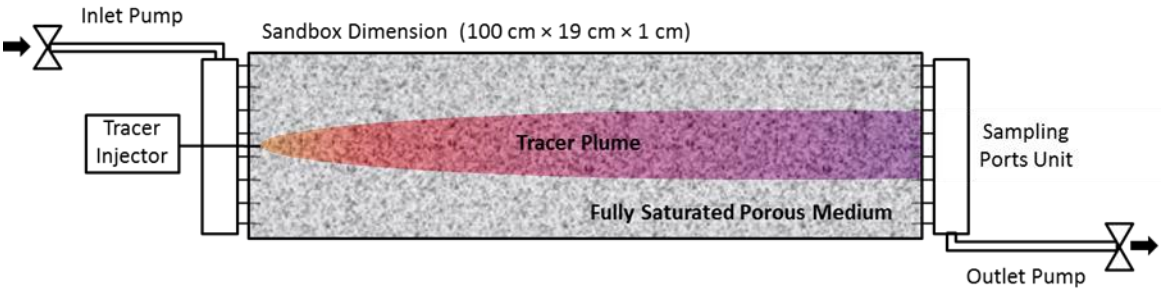

187

188 **Figure 1.** Schematic of the 2D flow and transverse disperison experiment conducted by Rolle et al.
189 (2013).

190

191 Using PHREEQC, Rolle et al. (2013) solved the problem numerically by simulating transverse
192 dispersion and electromigration perpendicular to the flow path as a 1D problem. This approach
193 simplifies a 2D steady-state problem into a 1D transient problem by making use of the
194 transformation t = x/v, where x is the distance from the source for the 2D problem, v is the
195 uniform average linear groundwater velocity, and t defines the travel time to reach the location x.
196 At the same time, t defines the simulation time for the 1D transient transverse dispersion problem
197 (Rolle et al., 2013). Coinciding with experimental conditions, a 1 cm source in the middle of the
198 12 cm wide cross section at x = 0 describes the continuous release of the electrolyte solution. The
199 simulation was run for the case of an average linear velocity of 1.5 m day^{-1}. The results of the
200 1D transient simulations are compared among the three participating codes, whereas fully 2D
201 simulations with explicit treatment of flow were performed with CrunchFlow and MIN3P.

202
203 **Table 4.** Chemical conditions and transverse dispersion coefficients for Benchmark 3 (transverse
204 dispersion problem).

Species	Tracer Injection Ports (mM)	Initial Condition (1D) and Remaining Injection Ports (2D) (mM)	Diffusion Coefficient (m^2 s^{-1})	Transverse Dispersion Coefficient (m^2 s^{-1})
K^+	0.29	10^{-6}	1.77×10^{-9}	2.405×10^{-9}
Mg^{2+}	0.29	10^{-6}	6.26×10^{-10}	1.745×10^{-9}
Cl^-	0.87	3×10^{-6}	1.81×10^{-9}	2.425×10^{-9}

The dispersion coefficients used in these simulations require some discussion. In fact, the parameterization of the hydrodynamic transverse dispersion coefficient used in Rolle et al. (2013) differs from the classical linear model commonly adopted in subsurface applications of solute transport and reads as:

$$D_i^T = D_i^P + D_i^{aq}\left(\frac{Pe^2}{Pe + 2 + 4\delta^2}\right)^{\beta} \quad (5)$$

where D_i^P is the pore diffusion coefficient approximated as the product of the aqueous diffusion coefficient of a species *i* and the porosity of the medium (0.41). $Pe=vd/D_i^{aq}$ is the grain Péclet number where *d* is the average grain size (1.25 mm). δ=6.2, and β=0.47 are empirical parameters determined in previous multitracer experiments and pore-scale simulations (Rolle et al., 2012). Equation 7 explicitly retains a direct dependence of the mechanical dispersion term on the aqueous diffusivity of the transported species; the non-linear dependence on the average flow velocity arises from the incomplete mixing in the pore channels (e.g. Hochstetler et al., 2013; Rolle and Kitanidis, 2014).

For this benchmark analysis we considered the mixed electrolyte case described in Rolle et al., 2013, where a dilute solution of KCl and $MgCl_2$ was continuously injected in ambient deionized water. The free aqueous diffusion coefficients of the ions at T=20 ºC are $D_{K+} = 1.77 \times 10^{-9}$ m^2 s^{-1}, $D_{Mg2+} = 6.26 \times 10^{-10}$ m^2 s^{-1}, and $D_{Cl-} = 1.81 \times 10^{-9}$ m^2 s^{-1}. These values used in Eq. 7 yield the transverse dispersion coefficients given in the last column of **Table 4**.

1D Benchmark: The 1D benchmark consists of a pure transverse diffusion problem discretized into 48 grid cells of 2.5 mm. In the 1D system, the injection ports constitute initial conditions used at grid cells 23-26, corresponding to a 10 mm wide region in the center of the symmetrical

system. The initial condition is used everywhere else in the domain and is intended to represent deionized water. The transverse dispersion coefficients given in **Table 4** are used. The boundaries at either end of the system are treated as no-flux, but they do not influence the system behavior for the 16 hour simulation time (corresponding to x = 1 m, i.e. the outflow boundary of the domain). The simulation was run with a constant 0.001 hour time step.

2D Benchmark: For the full 2D problem solved with CrunchFlow and MIN3P, the transverse discretization is 50 grid cells with a spacing of 2.4 mm (corresponding to a total width of 0.12 m). At the inlet boundary, grid cells 24, 25, 26 and 27 in the transverse direction are set at the tracer injection port concentrations of 0.29 mM K^+, 0.29 mM Mg^{2+}, and 0.87 mM Cl^- (see **Table** 4), while the remaining injection ports carry deionized water. The longitudinal discretization is 500 grid cells with a spacing of 2.4 mm thus a total length of 1.2 m; the concentrations are reported at x = 1.0 m, corresponding to the outflow boundary of the experimental setup. The additional length of 0.2 m is considered in the models to avoid any possible boundary effects. In this case, lateral flow can be calculated, or simply prescribed at 1.5 m day^{-1}. A maximum time step of 1 hour is used with an initial minimum time step of 10^{-6} hours. The simulation time is 32 hours to ensure that the final results correspond to steady state conditions representative of the experiment.

5. Results and Discussion

Benchmark 1

Simulation results for the Benchmark 1 (Lichtner, 1995) depict the diffusion of HNO_3 (pH = 4.007) from the solution domain towards the boundary where NO_3^- concentration are 100 times lower and pH = 6.001. Results for NO_3^- and H^+ reveal that both ions continue to diffuse towards

the left boundary after 1 hour simulation time (**Figure** 2). Because the diffusion coefficient for H^+ is much larger than the corresponding value for NO_3^-, H^+ has become substantially more depleted in the domain than NO_3^-. The discrepancy in diffusion rates of H^+ and NO_3^- triggered electromigration of Na^+ and Cl^- to maintain local charge balance; Na^+ is entering the domain to offset the preferential loss of H^+, while Cl^- is leaving the system to counterbalance NO_3^-, which is preferentially retained. Migration of Na^+ and Cl^- occurs despite the fact that there was no initial concentration gradient of either species (**Table 2**) and takes place even against the developing concentration gradients of Na^+ and Cl^-. If Fick's Law were used to describe this multispecies diffusion problem, there would be no change in Na^+ and Cl^- concentration and consequently electroneutrality would be violated.

There is very good agreement between the simulation results of all three codes and they demonstrate near identical outputs. Simulations were executed on a desktop computer equipped with an Intel Core 2 Quad CPU with two 2.4 GHz processors, 8 GB RAM and a 64-bit operating system.

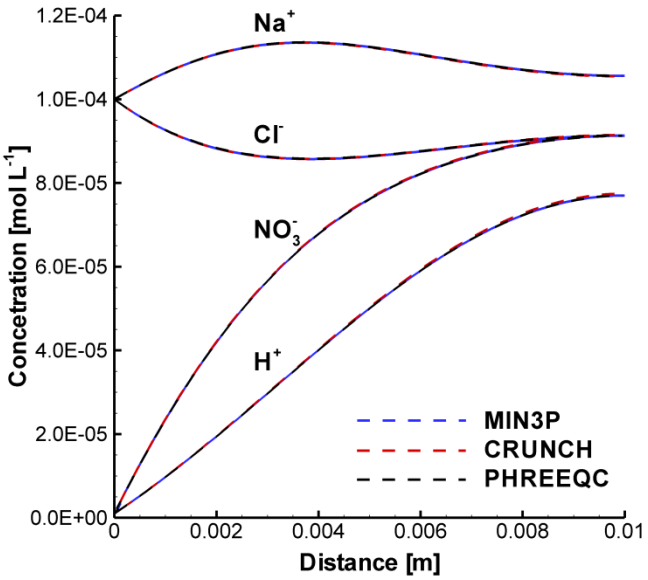

Figure 2: Species concentrations after 1 hour simulation time for HNO_3 diffusion (Benchmark 1). The left boundary is a fixed concentration (Dirichlet) boundary, while the right boundary is no-flux.

Benchmark 2

The results of the Benchmark 2 simulation visually show steady state diffusion with same concentration profiles for Na^+ and Cl^- from left to right (**Figure** 3). However, it has to be kept in mind that the diffusion coefficient for Cl^- is considerably larger than the one for Na^+. In fact, considering that the equations are based on the null current assumption, this holds back Cl^- migration and accelerates Na^+ migration. Although there are no initial concentration gradients for $^{22}Na^+$, H^+ and OH^-, these species, present at much lower concentrations, also become affected by the electrostatic coupling.

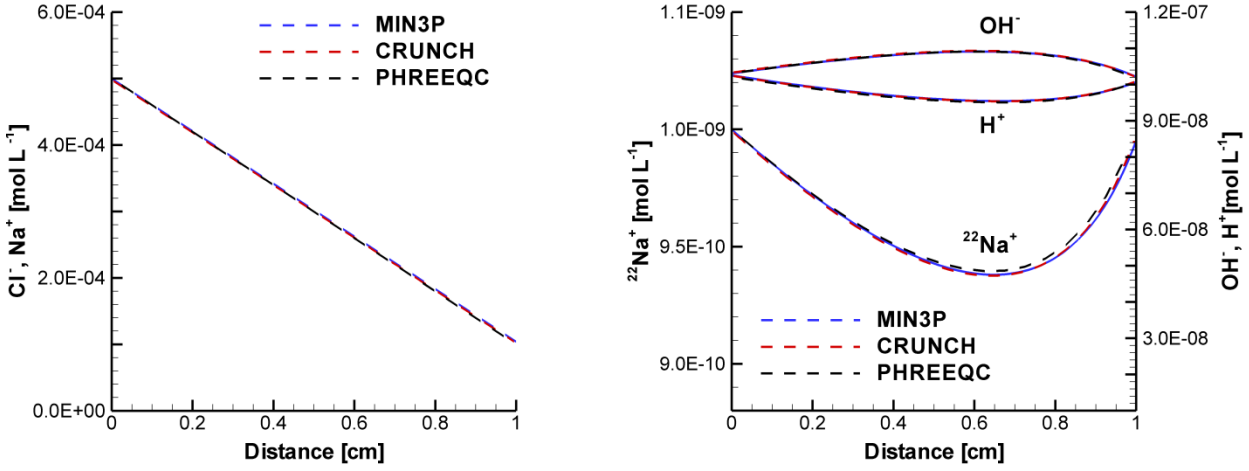

Figure 3: Na^+, Cl^-, H^+, OH^- and $^{22}Na^+$ concentrations after 1500 days for system summarized in Table 2 (Benchmark 2). The left boundary is a fixed concentration (Dirichlet) boundary at 0.5 mM, while the right boundary is a fixed concentration boundary at 0.1 mM for Na^+, Cl^-. The fixed gradient in NaCl results in a flux of H^+, OH^- and $^{22}Na^+$, despite the fact that their concentrations are the same at either end of the column.

285 A closer look at the results reveals that H^+ migrates from the left to the right to enhance the
286 positive charge flux, while OH^- migrates from the right to the left to counteract the negative
287 charge flux from the left to the right dominated by Cl^-. Primarily, one would expect that $^{22}Na^+$
288 should also be subjected to a net flux from the left to the right; however, the sodium isotope is
289 present at very low concentrations and is more strongly affected by migration dynamics of H^+
290 and OH^-, resulting in a net migration form the right to the left inducing an unexpected isotope
291 fractionation. Solving this problem with Fick's law would not predict $^{22}Na^+$ isotope fractionation,
292 H^+ and OH^- migration, and would result in a net negative charge flux across the domain. These
293 results suggest that multicomponent diffusion can introduce isotope fractionation, even in the
294 absence of fractionating reactions.
295 Overall, there is very good agreement between the three codes with better agreement between
296 CrunchFlow and MIN3P. Slight differences are observed for the PHREEQC results. It is difficult
297 to decisively determine the reasons for these differences, but it is likely that the discrepancies are
298 due to slight variations in model formation (i.e. consideration of activity gradients in the
299 PHREEQC formulation, absent in the other two codes) and/or the use of different coupling
300 schemes (GIM vs. SNIA). However, all codes show identical trends and concentration
301 differences are small, implying that the residual discrepancies will not affect the interpretation of
302 the results.
303

304 **Benchmark 3: 1D Transverse Dispersion**

305 The transverse concentration profiles for Cl^-, K^+ and Mg^{2+} are plotted at the outlet (x = 1.0 m)
306 corresponding to a residence time of 16 hours in the 2D domain. The separation of the three
307 tracer profiles (

Figure 4) demonstrates the effect of species-dependent dispersion coefficients and electrochemical migration on transverse displacement. The Cl^- concentration profile is located between K^+ and Mg^{2+} despite having the largest diffusion coefficient. In fact, D_{Cl^-} in liberated state is considerably larger than D_{Mg2+} and also slightly larger than D_{K+} (**Table 4**). These results show that Cl^- migration is retarded due to electrostatic coupling with the cations and in particular with Mg^{2+}, which diffuses more slowly. The outcomes reported in Fig. 4 demonstrate the positive contribution of electromigration to transverse displacement of the two cations and the negative contribution of electromigration to transverse displacement of chloride (Rolle et al., 2013).

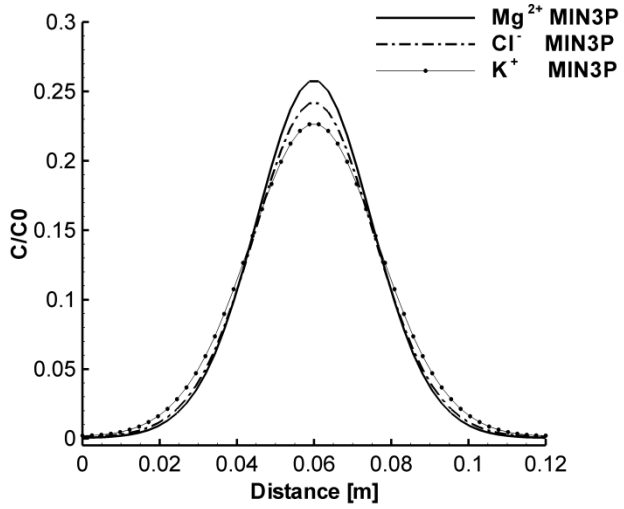

Figure 4. 1D simulation results of transverse profiles for Cl^-, K^+ and Mg^{2+} at the outlet (corresponding to a residence time of 16 hours) demonstrate the effect of species-dependent dispersion and electromigration on the transverse displacement of charged species (1D Benchmark 3 solved with MIN3P).

There is a very good agreement between the three codes and an excellent match between CrunchFlow and MIN3P (

Figure 5). Similar to the two previous benchmarks, there are slight differences between the results of CrunchFlow and MIN3P on the one hand and PHREEQC on the other hand. Peak chloride concentrations predicted by PHREEQC are slightly higher than those calculated by CrunchFlow and MIN3P (~ 0.6%). Magnesium and potassium concentration profiles are in very good agreement for all codes.

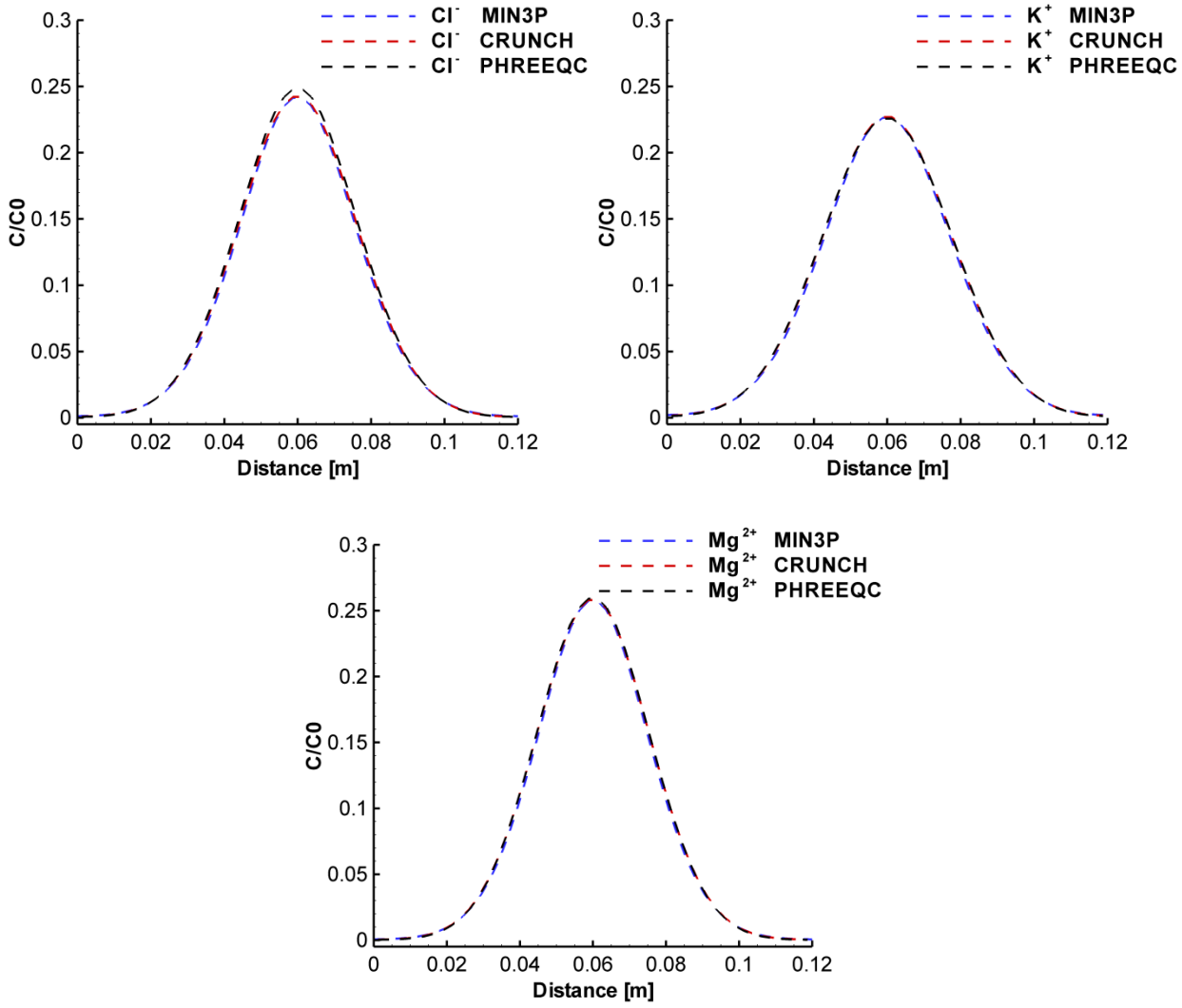

Figure 5. 1D simulation of transverse multicomponent diffusion for the case of transport of mixed electrolytes (KCl and $MgCl_2$ solution) in pure water described by Rolle et al. (2013), comparing CrunchFlow, MIN3P and PHREEQC results.

Benchmark 3: 2D Flow and Transverse Dispersion

Using CrunchFlow and MIN3P it was possible to carry out a full two-dimensional flow and multicomponent transport simulation of the flow-through system. The simulation was run for two pore volumes (32 hours) to ensure that steady state conditions at the outflow were reached. To illustrate the 2D concentration distributions and to provide a means for visual comparison of the CrunchFlow and MIN3P results, 2D contour plots are provided for K^+, Mg^{2+} and Cl^- (**Figure 6**).

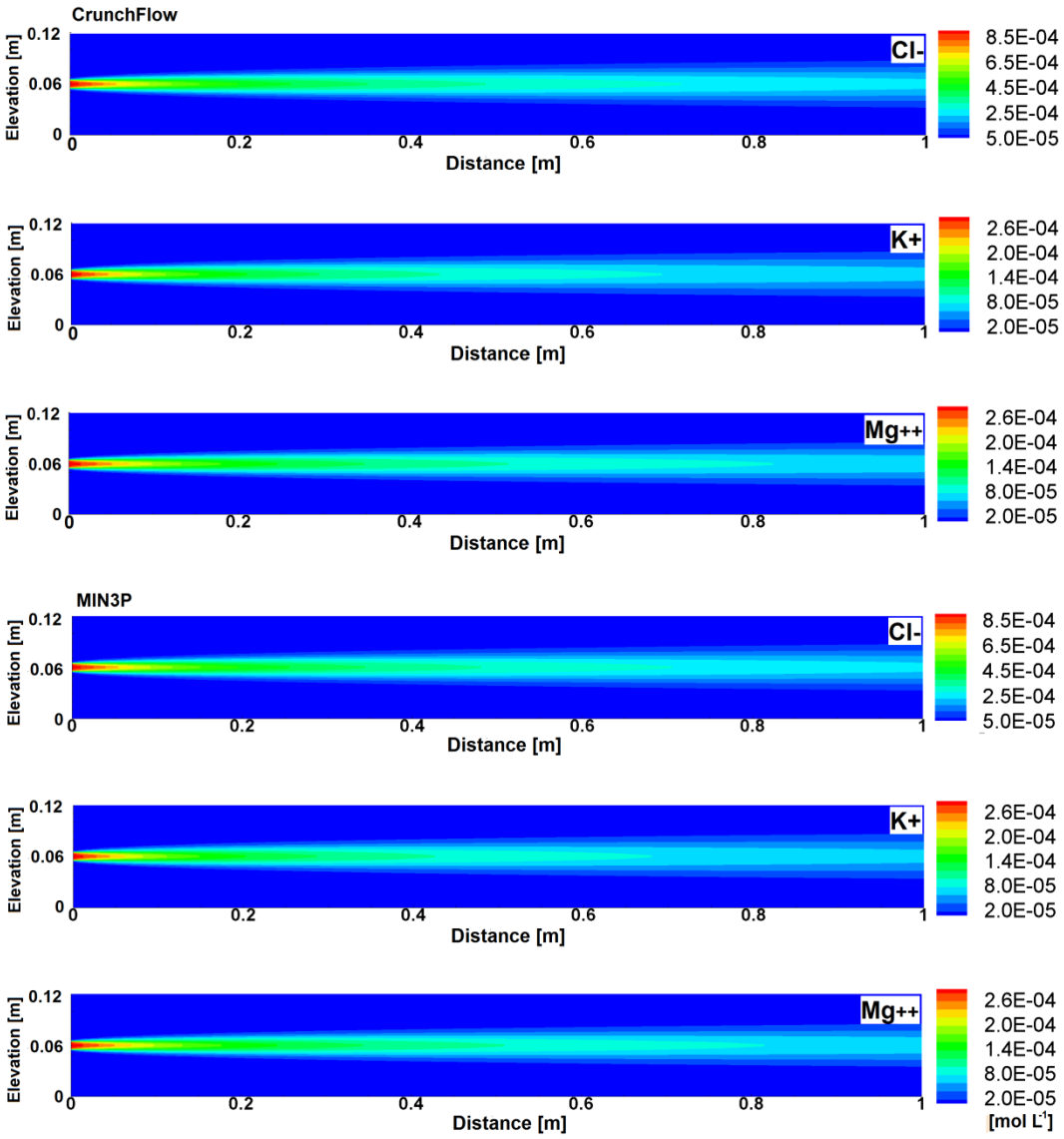

Figure 6. Simulation results for Benchmark 3 considering flow (uni-directional) and multicomponent transverse dispersion for steady-state conditions, from top to bottom are shown: K^+, Mg^{2+} and Cl^- for CrunchFlow and K^+, Mg^{2+} and Cl^- for MIN3P.

Cross-sections extracted from two-dimensional steady state CrunchFlow and MIN3P results are compared at the outflow to one-dimensional transient PHREEQC results, corresponding to a residence time of 16 hours. Overall, there is an excellent agreement between MIN3P and CrunchFlow results (**Figure 7)** and results are also very close to the concentrations computed with the 1D PHREEQC approach. PHREEQC concentration profiles are slightly higher than CrunchFlow

and MIN3P (the differences of the peak concentrations are ~ 0.6% for Cl^-, ~ 0.7% for Mg^{2+} and ~ 0.4% for K^+).

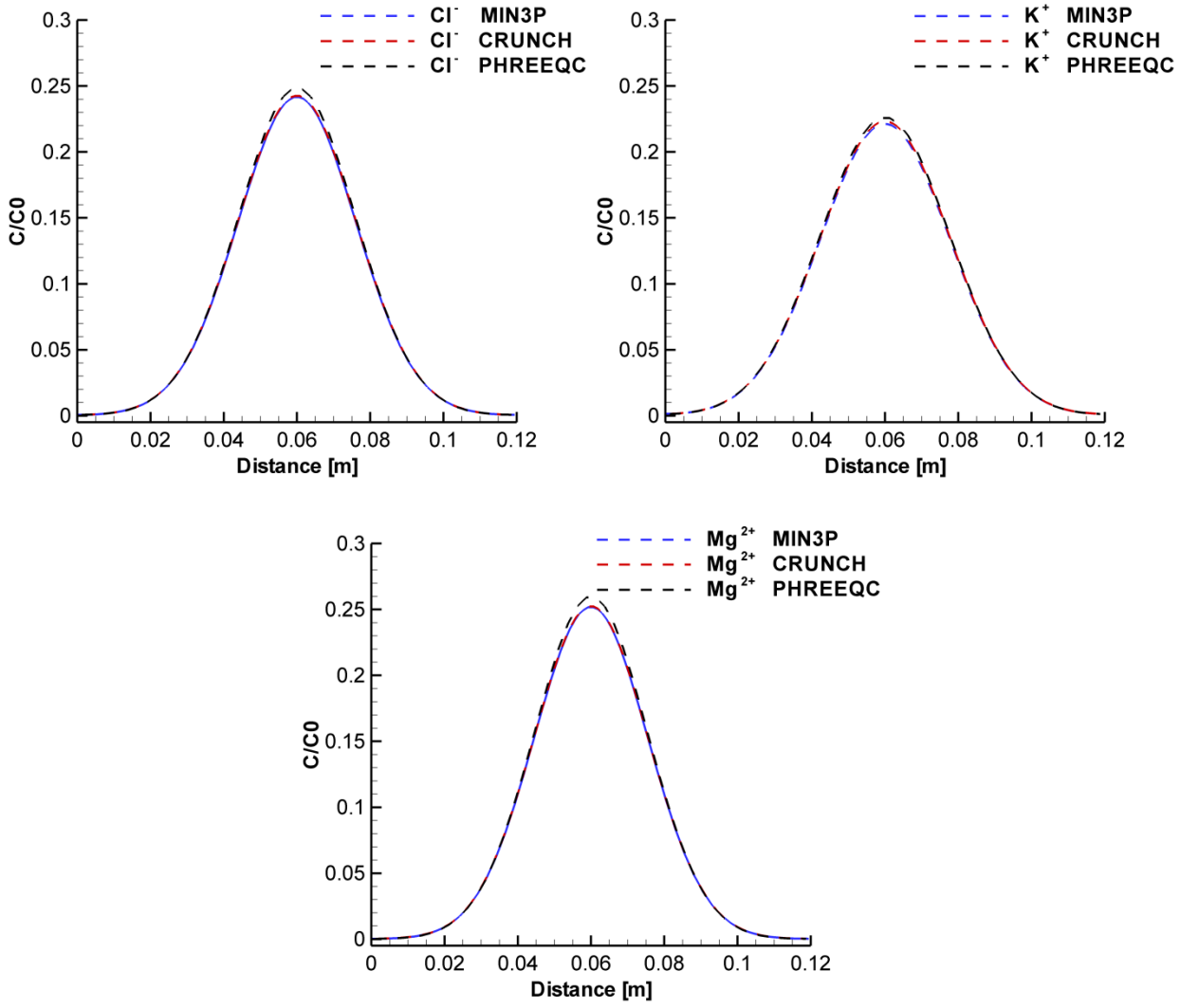

Figure 7. Comparison of 1D PHREEQC results (no explicit consideration of flow, only following the plume as it moves down the flow path) and transverse profiles derived from 2D CrunchFlow and MIN3P runs for the transverse dispersion problem. The CrunchFlow 2D runs are based on GIMRT and use a first order upwind formulation, along with a backwards Euler time stepping approach, the same numerical methods are used in the MIN3P simulations.

6. Concluding Remarks

Three benchmark problems were presented, each with significant effects of multicomponent diffusion and electromigration on transport of solutes in saturated porous media. The benchmarks were specifically designed to be sensitive to the effect of electromigration on diffusion and lateral concentration displacement. Benchmarks 1 and 2 are hypothetical problems that provide opportunities to verify the implementation of multicomponent diffusion and electromigration formulations in reactive transport codes. Benchmark 3 is based on the outcomes of laboratory experiments (Rolle et al., 2013) and provides the opportunity to verify and validate multicomponent diffusion and species-dependent transverse dispersion formulations under flow-through conditions. Three reactive transport codes with the capability of simulating multicomponent diffusion and electrochemical migration participated in this study (CrunchFlow, MIN3P and PHREEQC). For all benchmark problems considered in this work an overall very good agreement between the simulation results obtained with the different codes. Despite some residual discrepancies between the simulation results, all three codes were able to consistently reproduce the same trends and evolution in concentration patterns induced by multicomponent diffusion and by the electrostatic interactions between the charged species. Small discrepancies between the results indicate that different approaches in implementing the governing equations are not a significant source of uncertainties for model applications; uncertainties will rather be dominated by the underlying conceptual model.

Acknowledgements:

Funding for this research was provided by the Natural Sciences and Engineering Research Council of Canada (NSERC) in form of a Discovery Grant and a Discovery Accelerator

Supplement Award held by K. Ulrich Mayer. The contribution of C. Steefel was supported by the Director, Office of Science, Office of Basic Energy Sciences, Chemical Sciences, Geosciences, and Biosciences Division, of the U.S. Department of Energy under Contract No. DE-AC02-05CH11231. M. Rolle acknowledges the support of the Baden-Württemberg Stiftung under the Eliteprogram for postdocs.

References:

1. Alt-Epping, P., Tournassat, C., Rasouli, P., Steefel, C., Mayer, K., Jenni, A., Mäder, U., Sengor, S., Fernandez, R.: Benchmark reactive transport simulations of a column experiment in compacted bentonite with multispecies diffusion and explicit treatment of electrostatic effects. Comput. Geosci. (2015). doi:10.1007/s10596-014-9451-x

2. Appelo, C.A.J.:Multicomponent diffusion in clays. In: Candela, L., Vadillo, I., Aagaard, P. (eds.) Water Pollution in Natural Porous Media, pp. 3–13. Instituto Geologico de Espana, Madrid (2007)

3. Appelo, C.A.J., Wersin, P.: Multicomponent diffusion modeling in clay systems with application to the diffusion of tritium, iodide, and sodium in Opalinus Clay. Environ. Sci. Technol. 41, 5002–5007 (2007)

4. Appelo, C.A.J., Van Loon, L.R., Wersin, P.: Multicomponent diffusion of a suite of tracers (HTO, Cl, Br, I, Na, Sr, Cs) in a single sample of Opalinus Clay. Geochim. Cosmochim. Acta 74, 1201–1219 (2010)

5. Bagotsky, V.S.: Fundamentals of Elechtrochemistary, 2nd edn. John Wiley and Sons, Pennington (2006)

6. Bard, A.J., Faulkner, L.R.: Electrochemical Methods: Fundamentals and Applications. John Wiley and Sons, New York (1980)

7. Ben-Yaakov, S.: Diffusion of seawater ions—significance and consequences of cross coupling effects. Am. J. Sci. 281, 974–980 (1981)

8. Boudreau, B.P.: Diagenetic models and their implementation. Springer, New York (1997)

9. Boudreau, B.P., Meysman, F.J.R., Middelburg, J.J.: Multicomponent ionic diffusion in porewaters: Coulombic effects revisited. Earth Planet. Sci. Lett. 222, 653–666 (2004)

10. Carrera, J., Sanchez-Vila, X., Benet, I., Medina, A., Galarza, G., Guimera, J.: On matrix diffusion: formulations, solution methods and qualitative effects. Hydrogeol. J. 6, 178–190 (1998)

11. Chiogna, G., Cirpka, O.A., Grathwohl, P., Rolle, M.: Relevance of local compound-specific transverse dispersion for conservative and reactive mixing in heterogeneous porous media.Water Resour. Res. 47, W06515 (2011). doi:10.1029/2010WR010270

12. Cussler, E.L.: Diffusion: Mass Transfer in Fluid Systems, 2nd edn. Cambridge University Press, New York (1997)

13. Giambalvo, E.R., Steefel, C.I., Fisher, A.T., Rosenberg, N.D., Wheat, C.G.: Effect of fluid-sediment reaction on hydrothermal fluxes of major elements, eastern flank of the Juan de Fuca Ridge. Geochim. Cosmochim. Acta 66, 1739–1757 (2002)

14. Glaus, M.A., Birgersson, M., Karnland, O., Van Loon, L.R.: Seeming steady-state uphill diffusion of 22Na+ in compacted montmorillonite. Environ. Sci. Tech. 47, 11522–11527 (2013)

15. Helfferich, F.: Ion Exchange, 2nd edn. McGraw-Hill, NewYork (1962)

16. Hochstetler, D.L., Rolle, M., Chiogna, G., Haberer, C.M., Grathwohl, P., Kitanidis, P.K.: Effects of compound-specific transverse mixing on steady-state reactive plumes: insights from porescale simulations and Darcy-scale experiments. Adv.Water Resour. 54, 1–13 (2013). doi:10.1016/j.advwatres.2012.12.007

17. Johannesson, B., Yamada, K., Nilsson, L.O., Hosokawa, Y.: Multispecies ionic diffusion in concrete with account to interaction between ions in the pore solution and the cement hydrates. Materials and Structures, Kluwer Academic Publishers, 40, 651–665 (2007)

18. Kang, Q., Lichtner, P.C., Zhang, D.: Lattice Boltzmann porescale model for multi-component reactive transport in porous media. J. Geophys. Res 111, B05203 (2006). doi:10.1029/2005JB003951

19. LaBolle, E.M., Fogg, G.E.: Role of molecular diffusion in contaminant migration and recovery in alluvial aquifer system. Transp. Porous Media 42, 155–179 (2001)

20. Lasaga, A.C.: Treatment ofmulticomponent diffusion and ion-pairs in diagenetic fluxes. Am. J. Sci. 279, 324–346 (1979)

21. Lichtner, P.C.: Principles and practice of reactive transport modeling. Mater. Res. Soc. Symp. Proc. 353, 117–130 (1995)

22. Lichtner, P.C.: Continuum formulation of multicomponent–multiphase reactive transport. Ch. 1 in. reactive transport in porous media. In: Lichtner, P.C., Steefel, C.I., Oelkers, E.H. (eds.) Reviews in Mineralogy, vol. 34. Mineralogical Society of America, Washington, DC (1996)

23. Liu, C.X., Shang, J., Zachara, J.M.: Multispecies diffusion models: a study of uranyl species diffusion.Water Resour. Res. 47, W12514 (2011). doi:10.1029/2011WR010575

24. MacQuarrie, K.T.B., Mayer, K.U.: Reactive transport modeling in fractured rock: a state-of-the-science review. Earth Sci. Rev. 72, 189–227 (2005)

25. Mayer, K.U., Frind, E.O., Blowes, D.W.: A numericalmodel for the investigation of reactive transport in variably saturated media using a generalized formulation for kinetically controlled reactions.Water Resour. Res. 38, 1301–1321 (2002). doi:10:1029/2001WR000862

26. McDuff, E.R., Ellis, A.R.: Determining diffusion-coefficients in marine-sediments—laboratory study of the validity of resistivity techniques. Am. J. Sci. 279, 666–675 (1979)

27. Molins, S., Trebotich, D., Steefel, C.I., Shen, C.: An investigation of the effect of pore scale flow on average geochemical reaction rates using direct numerical simulation. Water Resour. Res. 48, W03527 (2012). doi: 10.1029/2011WR011404

28. Muniruzzaman, M., Haberer, C.M., Grathwohl, P., Rolle, M.: Multicomponent ionic dispersion during transport of electrolytes in heterogeneous porous media: experiments and model-based interpretation. Geochim. Cosmochim. Acta 141, 656–669 (2014)

29. Newman, J.S.: Electrochemical Systems. Prentice-Hall, Englewood Cliff (1973)

30. Oelkers, E.H.: Physical and chemical properties of rocks and fluids for chemical mass transport calculations. Rev. Mineral. Geochem. 34, 131–191 (1996)

31. Ovaysi, S., Piri, M.: Pore-scale dissolution of CO2+SO2 in deep saline aquifers. Int. J. Greenh. Gas Control 15, 119–133 (2013)

32. Parkhurst, D.L., Appelo, C.A.J.: User's guide to PHREEQC (version 2)—a computer program for speciation, batch-reaction, onedimensional transport, and inverse geochemical calculations. Denver (1999)

33. Paz-Garcia, J.M., Johannesson, B., Ottosen, L.M., Ribeiro, A.B.., Rodriguez-Maroto, J.M.: Modeling of electrokinetic processes by finite element integration of the Nernst-Planck-Poisson system of equations. Sep. Purif. Technol. 79, 183–192 (2011)

34. Rolle, M., Hochstetler, D.L., Chiogna, G., Kitanidis, P., Grathwohl, P.: Experimental investigation and pore-scale modeling interpretation of compound-specific transverse dispersion in porous media. Transp. Porous Media 93, 347–362 (2012)

35. Rolle, M., Muniruzzaman, M., Haberer, C.M., Grathwohl, P.: Coulombic effects in advection-dominated transport of electrolytes in porous media: multicomponent ionic dispersion. Geochim. Cosmochim. Acta 120, 195–205 (2013)

36. Rolle, M., Chiogna, G., Hochstetler, D.L., Kitanidis, P.K.: On the importance of diffusion and compound-specific mixing for groundwater transport: an investigation from pore to field scale. J. Contam. Hydrol. 153, 51–68 (2013)

37. Rolle,M., Kitanidis, P.K.: Effects of compound-specific dilution on transient transport and solute breakthrough: a pore-scale analysis. Adv. Water Resour. 71, 186–199 (2014)

38. Shiba, S., Hirata, Y., Seno, T.: Mathematical model for hydraulically aided electrokinetic remediation of aquifer and removal of nonanionic copper. Eng. Geol. 77, 305–315 (2005)

39. Steefel, C.I., Carroll, S.A., Zhao, P., Roberts, S.: Cesium migration in Hanford sediment: a multisite cation exchange model based on laboratory transport experiments. J. Contam. Hydrol. 67, 219–246 (2003)

40. Steefel, C.I., Maher, K.: Fluid-rock interaction: a reactive transport approach. Rev. Mineral. Geochem. 70, 485–532 D2009]. Mineralogical Society of America

41. Steefel, C.I., Appelo, C.A.J., Arora, B., Jacques, D., Kalbacher, T., Kolditz, O., Lagneau, V., Lichtner, P.C., Mayer, K.U., Meeussen, J.C.L.,Molins, S.,Moulton, D., Shao, H., Šimůnek, J., Spycher, N., Yabusaki, S.B., Yeh, G.T.: Reactive transport codes for subsurface environmental simulation. Comput. Geosci. (2014). doi:10.1007/s10596-014-9443-x

42. Taylor, R., Krishna, R.: Multicomponent Mass Transfer. John Wiley and Sons, New York (1993)

43. Tyrrell, H.J.V.: Diffusion and Heat Flow in Liquids. Butterworths, London (1961)

44. Van Cappellen, P., Gaillard, J.F.: Biogeochemical dynamics in aquatic sediments. Ch. 8 in.: reactive transport in porous media. In: Lichtner, P.C., Steefel, C.I., Oelkers, E.H. (eds.) Reviews in Mineralogy, vol. 34, pp. 335–376. Mineralogical Society of America, Washington, DC (1996)

45. Vinograd, J.R., McBain, J.W.: Diffusion of electrolytes and of the ions in their mixtures. J. Am. Chem. Soc. 63, 2008–2015 (1941)

46. Wang, Y., Van Cappellen, P.: A multicomponent reactive transport model of early digenesis: application to redox cycling in coastal marine sediments. Geochim. Cosmochim. Acta 60, 2993–3014 (1996)